Insight into the structural hierarchy of the protease cascade that regulates the mosquito melanization response

Sally A. Saab[a,b], Xiufeng Zhang[c], Bianca Morejon[c], Kristin Michel[c] and Mike A. Osta[a]

[a] Department of Biology, American University of Beirut, Beirut, Lebanon

[b] Current address: Department of Molecular Microbiology and Immunology, Johns Hopkins University, Baltimore, USA

[c] Division of Biology, Kansas State University, Manhattan, KS, USA

Short title: The protease cascade regulating mosquito melanization

Corresponding Author:

Mike A. Osta

Biology Department

American University of Beirut

Bliss Street

Beirut, Lebanon

Tel: +961-1-350000 (Ext. 3909)

E-mail: mo07@aub.edu.lb

Number of tables: 3 online supplementary tables

Number of figures: 7 main figures and 3 online supplementary figures

Word count: 6930

Key words: *Anopheles gambiae*, mosquito innate immunity, clip domain serine protease cascades, melanization

Abstract

Serine protease cascades regulate important physiological processes during infection, from complement activation and coagulation in mammals to melanization and Toll pathway activation in insects. Key components of these cascades in insects are clip domain serine proteases (CLIPs) including the catalytic, clip domain serine proteases (cSPs) and the non-catalytic, clip domain serine protease homologs (cSPHs), both of which are essential for the proper functioning of these cascades. In the context of the melanization immune response of insects, CLIPs cascades converge on the activation cleavage of the zymogen prophenoloxidase to active phenoloxidase that initiates melanin biogenesis on microbial surfaces. While we have previously provided insight into the structural hierarchy of cSPHs in these cascades in the mosquito vector of malaria *Anopheles gambiae*, the hierarchy of cSPs as well as their functional interactions with cSPHs remain largely unknown. Here, we define partially the structural hierarchy of *An. gambiae* cSPs of the CLIPB family that are key factors in the melanization response and characterize their relative contributions to the anti-bacterial melanization response and to mosquito susceptibility to bacterial infections. Based on *in vivo* and *in vitro* assays that gauge the activation cleavage profiles of candidate CLIPs, we also propose that bidirectional interactions between cSPs and cSPHs regulate signal amplification and propagation in these cascades.

Introduction

CLIP domain serine proteases (CLIPs) function in cascades to regulate several insect immune responses, including the activation of the Toll signaling pathway [1, 2], melanization [3, 4] and the complement-like system [5]. The CLIP gene family includes the catalytic, clip domain serine proteases (cSPs) and non-catalytic, clip domain serine protease homologs (cSPHs). Mosquitoes are attractive models to study these cascades due to the significant expansion of the CLIP gene family in their genomes [6-9], the propensity of cSPHs to play key roles in regulating these cascades in different microbial contexts [10-14], and the fact that the immune responses triggered by these cascades influence mosquito resistance to entomopathogenic fungal biocontrol agents [10, 15] and malaria parasites that infect millions every year [16, 17]. The functional significance

of the CLIP gene family expansion in mosquitoes is still unclear, but posits a more complex organization and regulation of CLIP cascades in mosquitoes. Both, cSPs and cSPHs are produced as zymogens that require proteolytic cleavage at a specific site in the N-terminus of the protease domain or in the clip domain, respectively, to become functional [2, 18-22]. Certain cSPHs, however, have predicted cleavage activation sites in the N-terminus of the protease-like domain, similar to cSPs [6].

CLIPs function in cascades whose roles in immunity have been mainly addressed in the context of activation of Toll pathway and melanization. In *Drosophila*, the cascade initiates with the autoactivation of a modular serine protease (ModSp) downstream of pattern recognition receptors (PRRs), culminating in the activation of a series of cSPs including, in order, Grass, Hayan/Persephone and Spaetzle processing enzyme (Spe) which cleaves the cytokine-like molecule Spaetzle (Spz) leading to Toll activation [1, 23-25]. Toll can also be activated independent of ModSp by direct activation cleavage of a bait region in Persephone by microbial proteases [26, 27]. This cascade, however, branches downstream of Hayan and Persephone to regulate the fly's melanization response [1]. Two independent pathways control melanization in *Drosophila*; In response to Gram-positive bacteria, the extracellular protease cascade that regulate Toll activation branches downstream of Hayan/Persephone to activate Sp7 and prophenoloxidase 1 (PPO1), whereas, cuticular injury activates Hayan through an unknown mechanism leading to PPO1 and PPO2 activation [1]. In the tobacco hornworm *Manduca sexta*, the hemolymph proteinase 14 (HP14) functions as a ModSp and is autoactivated downstream of PRRs leading to the activation of the cSP HP21 [28]. Briefly, the cascade branches downstream of HP21 into two axes; one axis culminates in the activation of prophenoloxidase-activating protease 2 (PAP2) and PAP3 and two cSPHs (SPH1 and SPH2) leading to PPO activation, and the second culminates in the activation of HP6 which can further amplify the melanization response by cleaving PAP1 or activate Toll pathway by cleaving HP8, homolog of *Drosophila* Spe [28-32].

The genome of the malaria vector *An. gambiae* contains 110 CLIP genes, which are divided into 5 subfamilies; A, B, C, D and E [6, 9]. CLIPs B, C and D are predicted as catalytic cSPs, CLIPAs as non-catalytic cSPHs, whereas CLIPEs contain cSPHs or hybrid genes that encode proteins with both catalytic and non-catalytic protease domains. Genetic studies in *An. gambiae* identified several cSPHs as key regulators of the infection-induced melanization response. SPCLIP1 (CLIPA30; [6]), CLIPA8 and CLIPA28 form a core cSPH module that is central to the

melanization of *P. berghei* ookinetes in the basal labyrinth of the mosquito midgut epithelium and to the activation of hemolymph PPO in response to systemic bacterial infections [10, 12, 13, 33]. These cSPHs exhibit a clear hierarchy of activation cleavage in the hemolymph with SPCLIP1 being most upstream followed by CLIPA8 then CLIPA28 [10, 34]. So far, only the thioester-containing protein 1 (TEP1), a hallmark of mosquito humoral immunity, has been shown to act upstream of this cSPH module, controlling the activation cleavage of its constituent cSPHs [10, 34], whereas the identity of the cSPs that cleave the cSPHs in this module remain unknown. On the other hand, CLIPA2 and CLIPA14, act as negative regulators of *An. gambiae* melanization response as their knockdown dramatically enhances the melanization of *P. berghei* ookinetes and hemolymph PO activity in response to systemic bacterial infections [11, 14]. Interestingly, the core cSPH module controls the cleavage of CLIPA14, possibly as a negative feedback loop to regulate the intensity of melanization [11].

Three experimental models for melanization, *P. berghei* ookinete melanization in *CTL4* kd mosquitoes, melanotic tumor formation due to uncontrolled hemolymph PO activity in *serpin 2* (SRPN2) knockdown (kd) mosquitoes, and increase in melanotic excreta after bacterial challenge, have been used in genetic studies to identify several melanization-related cSPs of the CLIPB and C families, including CLIPB4, B8, B9, B10, B14, B17 and CLIPC9 [33-37]. Surprisingly, none of these cSPs seems to individually regulate proteolysis within the core cSPH module *in vivo* [10, 34], raising questions about the molecular interactions that control cSPH cleavage in mosquito CLIP cascades, especially because lepidopteran cSPs, specifically PAPs, are known to cleave key cSPHs during the melanization response [38-40]. Unlike cSPHs, the organization of *An. gambiae* cSPs in the protease cascade regulating melanization remains largely unknown, with the exception of CLIPB4, CLIPB9 and CLIPB10 which seem to function most downstream as PAPs, based on their ability to cleave *M. sexta* PPO *in vitro*, and CLIPB8, based on genetic data being upstream of CLIPB9 in the PPO activation cascade [35, 37, 41, 42]. Also, the individual contribution of these cSPs to the process of melanin formation in response to bacterial infections remains unexplored. Here, we define partially a hierarchical pattern of activation of the *An. gambiae* cSPs involved in melanization and characterize their relative contributions to this immune reaction in response to different bacterial challenges. Using *in vivo* functional genetic analysis and *in vitro* assays, we also provide novel insight into the functional organization of cSPs and cSPHs in the

protease cascade regulating mosquito melanization that advance our understanding of signal propagation and amplification in these cascades.

Materials and Methods

Anopheles gambiae *rearing*

Experiments were done using *Anopheles gambiae* G3 strain. Mosquitoes were reared in the insectary at 27 °C (± 0.5) and 80% (± 5%) humidity with a 12 h day-night cycle. Larvae were reared at low densities of approximately 100–120 larvae/pan of area 768 cm^2 and fed on TetraMin tropical fish food which was grinded into fine particles, while adults were given sugar pads containing 10% sucrose that was sterilized by autoclaving. Adult female mosquitoes were given BALB/c mice blood (mice were anaesthetized with ketamine) once per week for egg production. Alternatively, adult mosquitoes were fed on commercial horse blood using an artificial feeding system consisting of glass feeders covered with Parafilm and connected to a 37°C circulating waterbath.

Double Stranded RNA Synthesis and Gene Silencing

DNA amplification of the genes of interest was performed using the T7 flanked primers listed in online suppl. Table S1. Double stranded RNA (dsRNA) synthesis was performed from purified T7-tagged PCR amplicons using the T7 RiboMax Express Large-Scale RNA production system (Promega) according to the manufacturer's instructions. DsRNAs were extracted with Phenol:Chloroform:Isoamyl alcohol (25:24:1), followed by isopropanol precipitation and resuspension in nuclease-free water at a final concentration of 3.5 µg/µl. *In vivo* gene silencing by RNAi was performed as previously described [43]. Briefly, 1 to 3-days-old female adult mosquitoes were anesthetized under CO_2 and microinjected intrathoracically with 69 nl of a 3.5 µg/µl gene-specific dsRNA solution in water, using a Drummond Nanoject II nanoliter injector. Mosquitoes were allowed 2-4 days to recover before further manipulation.

Efficiency of gene silencing was measured by western blot analysis for most genes and by quantitative real time PCR (qRT-PCR) for *Rel1*, *CLIPB14* and *CLIPB17* due to the lack of a gene-specific antibody. To measure the efficiency of gene silencing at the protein level, hemolymph was extracted from approximately 40 naïve mosquitoes per genotype including, the ds*LacZ* control, at 3 to 4 days after dsRNA injection and proteins were quantified using Bradford Reagent (Fermentas). Equal amounts of proteins were resolved by reducing SDS-PAGE,

transferred to Immuno-blot PVDF membrane (Bio-Rad) using wet transfer (Bio-Rad) and subjected to western blot analysis with the appropriate antibody dilution (western blot section below). The gene silencing efficiency of *Rel1*, *CLIPB14* and *CLIPB17* was measured by qRT-PCR as follows. Total nucleic acids were extracted from 15 mosquitoes per genotype, including ds*LacZ*, using TRIzol reagent (Invitrogen), followed by extraction with Phenol:Chloroform:Isoamyl alcohol (25:24:1) and precipitation by isopropanol. Contaminant genomic DNA was removed by DNAse I (RNAse-free; Thermo Scientific) treatment as per the manufacturer's instructions. First-strand cDNA was produced from 1μg of total RNA using the iScript cDNA synthesis kit (Bio-Rad), as described by the manufacturer. qRT-PCR was performed in a CFX96 Real-Time Detection System (Bio-Rad) using SYBR Green JumpStart Taq ReadyMix (Sigma), according to the manufacturer's instructions. The *An. gambiae* ribosomal S7 gene was used as an internal control for normalization and relative gene expression values were calculated using the comparative C_T method. Primers used in qRT-PCR are listed in online suppl. Table S2.

Hemolymph cleavage profile of cSPs by western blot analysis

Wild type or dsRNA treated adult *An. gambiae* female mosquitoes were infected with the GFP-expressing, ampicillin-resistant *Escherichia coli* OP-50 strain (OD_{600}= 0.8 or 3) [44], the tetracycline resistant *Staphylococcus aureus* (OD_{600}= 0.8 or 1.5) [13] or *Beauveria bassiana* spores suspended in water (2000 spores/mosquito), prepared as described previously [45]. Hemolymph was extracted by proboscis clipping from groups of 40 mosquitoes per genotype in sterile 1x phosphate-buffered saline (PBS) containing a protease inhibitor cocktail (Roche), and protein concentration determined using Bradford protein quantification assay (Fermentas). Equal amounts of protein from the different hemolymph samples were resolved by SDS-PAGE and wet transferred using BioRad apparatus to immunoblot PVDF membranes that were blocked for 1 hr in 1x PBS containing 0.5% Tween 20 and 3% skimmed milk, then incubated with the appropriate primary antibody overnight at 4 °C. The primary antibodies included, rabbit αCLIPB4 (1:3000; produced by BOSTER), rabbit αCLIPB8 (1:1000;[41]), rabbit αCLIPB9 (1:1000; produced by BOSTER), rabbit αCLIPB10 (1:1000; [37]), rabbit αCLIPC9 (1:2000; kind gift from Michael Povelones, [34]), rabbit αCLIPA2 (1:1000; [14]), rabbit αCLIPA14 (1:3000, produced by BOSTER), mouse αCLIPA8 (1:100; [13]), rabbit αCLIPA28 (1:1000; [10]), rabbit αSPCLIP1 (1:2000; produced by BOSTER), rabbit αTEP1 (1:1000; [10]), rabbit

αSRPN2 (1:1000; [46]), mouse αApolipophorin II (1:100; [47]) and αCTL4 (1:1000; produced by Boster). Following washing, blots were incubated with anti-rabbit or anti-mouse IgG horseradish peroxidase-conjugated secondary antibodies at dilutions of 1:15000 or 1:6000, respectively. Western blots were revealed with BioRad Clarity Max western ECL substrate and imaged using ChemiDoc MP (BioRad).

Melanization-Associated Spot Assay (MelASA)

Mosquitoes were injected with dsRNA targeting LacZ (negative control), CLIPB4, CLIPB8, CLIPB9, CLIPB10, CLIPB14, CLIPB17 and SPCLIP1 (positive control). Two days post silencing, mosquitoes were injected with *Escherichia coli* OP-50 strain (OD_{600} =3; [44]), the tetracycline resistant *Staphylococcus aureus* strain (OD_{600} =3; [13]), or lyophilized *M. luteus* (ATCC, No. 4698, MilliporeSigma) resuspended in 1x PBS to an OD_{600}=5. Groups of 35 (for *E. coli* and *S. aureus* infections) or 50 (for *M. luteus* infections) infected mosquitoes per genotype were housed in carton cups containing clean, white Whatman filter papers (5.5 cm diameter) at the bottom. Twelve hours (for *E. coli* and *S. aureus*) and 18 hours (for *M. luteus*) post-infections, the filter papers containing melanin spots in mosquito fecal excretions were imaged under white epi-illumination without filters in a ChemiDoc MP (BioRad). Image processing and total spot area calculations were performed as described previously [34]. Experiments were repeated at least six times. Differences in Total melanotic spot area were analyzed using unpaired t-tests to compare two treatment groups, and One-Way ANOVA with Dunnett's post-test to compare multiple treatment groups in GraphPad Prism (version 9.5.1). Means were considered to differ significantly if $P < 0.05$.

Bacterial Proliferation and Mosquito Survival Assays

Mosquito resistance to bacterial infections was determined by scoring the Colony Forming Units (CFU) counts in whole mosquito homogenates. Briefly, dsRNA-treated adult female *An. gambiae* mosquitoes were injected intrathoracically with the *E. coli* OP-50 strain or the tetracycline resistant *S. aureus* strain suspended in 1x PBS at an OD_{600}=0.8. For each mosquito genotype, five to six batches of eight mosquitoes each were grinded in Luria Bertani (LB) broth at 24 hours post-infection, and serial dilutions of the homogenates were plated on LB agar plates supplemented with the appropriate antibiotics and incubated at 37 °C overnight. CFUs of the GFP-expressing *E. coli* OP-50 were counted under a fluorescent stereoscope since mosquito midguts naturally harbor ampicillin resistant bacteria. Results from at least five different

experiments were collected and analyzed using the Kruskal-Wallis test followed by the Dunn's multiple comparison test that compares mean ranks of each group to the ds*LacZ* control. Means of different groups were considered significantly different if the $P < 0.05$.

To score mosquito survival following bacterial challenge, dsRNA-treated mosquitoes were injected similarly with *E. coli* or *S. aureus* strains at OD_{600}= 0.8 and OD_{600}= 2 respectively. DsLacZ mosquitoes were used a negative control, while ds*CTL4* and ds*Rel1* mosquitoes were used as positive controls for *E. coli* and *S. aureus* infections, respectively. Mosquito survival was scored daily over two weeks. The Kaplan-Meier survival test was used to calculate percent survival. Experiments were repeated at least five times and the statistical significance of the observed differences was calculated using the Log-rank test. One representative experiment was shown.

In vitro *assays to study CLIPA8 cleavage by candidate CLIPBs*

To construct CLIPA8 expression vector, the sequence between BglII and PacI sites of pOET3 Transfer Plasmid (Oxford Expression Technologies) was replaced by a synthesized fragment (Integrated DNA Technologies), encoding Asp- Leu-V5 tag (GKPIPNPLLGLDST)-Arg- Thr- Gly-His tag (HHHHHH)-stop codon to produce plasmid pOET3-V5-His (online suppl. Table S3). To amplify the fragment encoding proCLIPA8 (AGAP010731), primers were synthesized flanking the full-length CLIPA8 including the predicted signal peptide, a NotI restriction site included before the start codon, and replacing the original stop codon by three consecutive Glycine codons (GGA) and a BglII site (online suppl. Table S3). The CLIPA8 fragment was amplified from the cDNA of adult female mosquitoes of *An. gambiae* G3 strain. CLIPA8 PCR amplicon and pOET3-V5-His were digested with NotI and BglII restriction enzymes (New England BioLabs), and ligated using T4 DNA ligase (Promega) to produce pOET3-CLIPA8-V5-His plasmid. To utilize the commercially available protease Factor Xa (New England BioLabs) for protein cleavage, the predicted cleavage site in CLIPA8 ^{63}IMLR^{66} was replaced by IEGR [35] using the CLIPA8mutag primer and the QuikChange Multi Site-Directed Mutagenesis Kit (Agilent Technologies) to create plasmid pOET3-CLIPA8$_{Xa}$-V5-His (online suppl. Table S3). Plasmids pOET3-CLIPA8-V5-His and pOET3-CLIPA8$_{Xa}$-V5-His were utilized to create the P0 viruses with FlashBAC Gold - Baculovirus Expression System (Genway Biotech), Sf9 cells and Cellfectin II Reagent (Gibco). Viruses were amplified and inoculated at

MOI of 1 for 800 ml of Sf9 suspension culture at 2×10^6 cells/ml in Sf-900II serum-free medium (Invitrogen). Expression media was harvested at 2 days post inoculation, and cells were cleared by centrifugation at 4000 rpm and 4 ℃ for 20 min. The clarified supernatant was dialyzed three times against 10 mM Na_2HPO_4 pH 8.0 and His-tagged CLIPA8 was purified over an Ni-NTA agarose column according to the manufacturer's instructions (Qiagen). Coomassie Brilliant blue (CBB) staining and Western blot using THE™ His Tag Antibody (GenScript) were performed to combine fractions containing the target protein. Pooled fractions were dialyzed twice against 20 mM Tris•HCl, 20 mM NaCl, pH 8.0, and subjected to purification over a 1.4-ml Q Sepharose Fast Flow column (Cytiva). Proteins were eluted with a linear gradient of 10-1000 mM NaCl in 20 mM Tris•HCl pH 8.0. CBB staining and Western blot using anti-His antibody were performed to screen fractions for the target protein. Recombinant protein was concentrated and buffer exchanged with 20 mM Tris•HCl, 50 mM NaCl, pH 8.0 using Amicon Ultra centrifugal filter units (Sigma-Aldrich). Purified proteins were confirmed by CBB staining and Western blot analyses using anti-His antibody, THE™ V5 Tag antibody (GenScript), and CLIPA8 primary antibody (Boster Biological Technology).

To study the cleavage of CLIPA8 by candidate CLIPBs, Factor Xa activation of proCLIPB4$_{Xa}$-His, proCLIPB9$_{Xa}$-His and proCLIPB10$_{Xa}$-His was performed similarly as described previously [35, 37, 41]. Briefly, for CLIPB4$_{Xa}$ and B10$_{Xa}$, 1 µg of purified recombinant zymogen was incubated overnight with 0.25 µg of commercial bovine Factor Xa (New England Biolabs) in a total volume of 10 µl of Factor Xa activation buffer (20 mM Tris•HCl, 100 mM NaCl, 2 mM $CaCl_2$, pH 8.0). For B9$_{Xa}$, 2 µg of zymogen was incubated overnight with 1 µg of Factor Xa in a total volume of 40 µl activation buffer. For each CLIPB activation, two negative controls were assembled in parallel, in which either Factor Xa or the zymogen was substituted by the same volume of buffer. B9$_{Xa}$ and B10$_{Xa}$ were activated at 37 ℃, and B4$_{Xa}$ was activated at RT. To assess the cleavage pattern of wild-type proCLIPA8-V5-His by B4, B9 and B10, a positive control was assembled including Factor Xa and proCLIPA8$_{Xa}$-V5-His. In a total volume of 40 µl activation buffer, 4 µg of proCLIPA8$_{Xa}$ was incubated at RT for 2 hours with 1 µg of Factor Xa. In parallel, two negative controls were set up by replacing Factor Xa or proCLIPA8$_{Xa}$-V5-His with the same volume of buffer. To examine the interaction of B9 and A8, 1 µl of proCLIPA8 (250 ng/µl) was mixed with 7.5 µl of Factor Xa-activated B9$_{Xa}$ (375 ng proCLIPB9$_{Xa}$) and 1.5 µl of reaction buffer 1 (20 mM Tris•HCl, 5 mM $CaCl_2$, pH 7.5), and

incubated at RT for 1 hour. For B4 with A8, 1 µl of proCLIPA8 (100 ng/µl) was mixed with 2 µl of Factor Xa-activated $B4_{Xa}$ (200 ng proCLIPB4_{Xa}) and 7 µl of reaction buffer 1, and incubated at RT for 1 hour. For B10 with A8, 1 µl of proCLIPA8 (100 ng/µl) was mixed with 1 µl of diluted Factor Xa-activated $B10_{Xa}$ (10 ng proCLIPB10_{Xa}, diluted with Factor Xa activation buffer) and 8 µl of reaction buffer 2 (20 mM Tris•HCl, pH 7.5), and incubated on ice for 30 min. For each CLIPB interaction with A8, three negative controls were assembled where Factor Xa-activated CLIPBs were replaced by the same volume of Factor Xa activation buffer only, CLIPB zymogen only, and Factor Xa only. Reactions were subjected to Western blot analyses using anti-His and anti-V5 antibodies.

Results

Systemic infections trigger the cleavage of CLIPB10 and consumption of CLIPB8

cSPs require proteolytic processing to become active according to biochemical studies in several insect species [28, 31, 32, 40, 48]. In *An. gambiae*, out of the 63 cSPs identified in the genome [6, 9], several CLIPB members including, CLIPB4, CLIPB8, CLIPB9, CLIPB10, CLIPB14, CLIPB17 were shown to play a significant role in *P. berghei* melanization in *CTL4* kd refractory mosquitoes and in melanotic tumor formation induced in naïve *SRPN2* kd mosquitoes [33-37]. In an effort to determine the hierarchical activation of these CLIPBs, we set out first to characterize their hemolymph cleavage profiles in response to infection, which may then be used as readouts to build hierarchy, as previously described for *An. gambiae* cSPHs [10, 34]. To that purpose, systemic infections were established in adult, female *An. gambiae* mosquitoes by intrathoracic injection of *B. bassiana* spores (2000 spores/ mosquito), *S. aureus* (OD_{600nm} = 3), or *E. coli* (OD_{600nm} = 3), and hemolymph extracts were obtained at different time points and subjected to western blot analysis with a panel of anti-CLIPB antibodies. No cleavage products were detected for CLIPB4 and CLIPB9 after septic infections with any of the microbial challenges despite challenging mosquitoes with high OD values (OD_{600}=3) (online suppl. Fig. S1). With respect to CLIPB8, its ~48kDa full-length form detected in the hemolymph of naïve mosquitoes was consumed completely at 24- and 10-hours following *B. bassiana* (Fig.1a) and *S. aureus* infections (Fig.1b), respectively, but was not altered by *E. coli* infections (Fig.1c). Full-length CLIPB10 (CLIPB10-F) of ~ 40 kDa was cleaved at later time points after *S. aureus* infections as indicated by the detection of a weak, lower molecular weight band (CLIPB10-C) of

~35 kDa (Fig. 1e), corresponding to the C-terminal protease domain (antibody was raised against the protease domain [37]). Interestingly, CLIPB10 cleavage was not detected after *B. bassiana* (Fig. 1d) nor *E. coli* (Fig. 1f) infections, suggesting that Gram-positive bacteria constitute a stronger stimulus for CLIPB10 cleavage. Unfortunately, we were not able to characterize CLIPB17 and CLIPB14 proteins since their custom-made antibodies failed to detect specific bands in the hemolymph.

CLIPB4 and CLIP17 act upstream of CLIPB8 and CLIPB10 in the protease cascade regulating melanization

We utilized CLIPB8 depletion and CLIPB10 cleavage patterns in the hemolymph of *S. aureus* infected mosquitoes as readouts to assign hierarchy among the CLIPBs involved in melanization. Silencing *CLIPB4* and *CLIPB17* rescued CLIPB8 depletion (Fig. 2a) and abolished CLIPB10 cleavage (Fig. 2b) in the hemolymph at 10 and 24 hrs after *S. aureus* infection, respectively (Fig. 2a), indicating that CLIPB4 and CLIPB17 act upstream of CLIPB8 and CLIPB10. The fact that *CLIPB8* kd did not abolish CLIPB10 cleavage and that *CLIPB10* kd did not rescue CLIPB8 depletion suggests that the cascade bifurcates downstream of CLIPB4 and CLIPB17 into two branches; one converging on CLIPB8 and the other on CLIPB10 (Fig. 2c). Interestingly, *SPCLIP1* silencing rescued infection-induced CLIPB8 depletion (Fig. 2a) and abolished CLIPB10 cleavage (Fig. 2b), further confirming its upstream position in the melanization response as part of the core [SPCLIP1-CLIPA8-CLIPA28] cSPH module [10, 34]. CLIPB8 silencing almost depleted CLIPB8 from the hemolymph (Fig. 2a), whereas CLIPB10 silencing significantly reduced CLIPB10 hemolymph levels, suggesting that CLIPB10 is either abundantly produced or that certain cell populations that express CLIPB10 show some resistance to RNAi. The silencing efficiencies of the remaining genes used in this assay are shown in online suppl. Fig. 2.

TEP1 and the core cSPH module are upstream regulators of CLIPBs in the melanization response

SPCLIP1, CLIPA8 and CLIPA28 form a core cSPH module exhibiting a clear hierarchy of activation cleavage with CLIPA28 being most downstream [10]. The fact that SPCLIP1 controlled the activation of CLIPB8 and CLIPB10, we asked whether the other two members of

the module exhibit a similar phenotype. Indeed, silencing either CLIPA8 or CLIPA28 abolished CLIPB10 cleavage (Fig. 3a) and rescued CLIPB8 depletion (Fig. 3b) in the hemolymph of *S. aureus* infected mosquitoes. These results, together with the reported observations that CLIPB4, CLIPB8, CLIPB9, CLIPB14, and CLIPB17 are individually dispensable for the proteolytic processing of CLIPA28 *in vivo* [10], and that the core cSPH module functions upstream of the catalytic CLIPC9 [34], strongly suggest that this module acts, upstream of all catalytic CLIPs with reported roles in *An. gambiae* melanization (Fig. 3c).

Only TEP1 has been shown to function upstream of the core cSPH module, as it is essential for the proteolytic processing of SPCLIP1 [12], CLIPA8 [10, 12] and CLIPA28 [10]. Hence, we asked whether TEP1 also regulates CLIPB8 and CLIPB10 activation during systemic infections. Indeed, TEP1 silencing abolished CLIPB10 cleavage (Fig. 3a) and rescued CLIPB8 depletion (Fig. 3b) in the hemolymph of *S. aureus* infected mosquitoes, placing TEP1 as the most upstream factor in the melanization response (Fig. 3c).

CLIPC9 is a member of the catalytic CLIPC family that was previously shown to function downstream of the core cSPH module in the melanization response [34]. Here, we show that *CLIPC9* kd rescued infection-induced CLIPB8 depletion (Fig. 3b) and abolished CLIPB10 cleavage (Fig. 2b) after *S. aureus* infections, suggesting that it acts upstream of these two CLIPBs. Although CLIPC9 is cleaved in response to systemic infections [34], we were not able to determine its placement with respect to CLIPB4 and CLIPB17 because we ran out of CLIPC9 antibody towards the end of the project.

CLIPA2 and CLIPA14 are potent negative regulators of the melanization response, whose knockdown triggers an enhanced melanotic response against *P. berghei* ookinetes and bacteria [11, 14, 33]. Also, SRPN2 negatively regulates mosquito melanization by targeting several catalytic CLIPs in the cascade [10, 34, 41]. The knockdown of neither of these negative regulators influenced CLIPB10 cleavage (Fig. 3a) and CLIPB8 consumption (Fig. 3b) patterns in the hemolymph; although *CLIPA2* kd appears to enhance CLIPB10 cleavage, this phenotype was not consistently observed (data not shown).

CLIPA8 is cleaved by several CLIPBs in vitro

It is surprising that only TEP1 silencing, so far, has been shown to block the proteolytic processing of members of the core cSPH module in response to systemic microbial infections

[10, 12], whereas, silencing none of the key cSPs (of the CLIPB and CLIPC families) involved in mosquito melanization was able to phenocopy TEP1 [10, 34]. We hypothesize that several cSPs may cleave the same cSPH to trigger the rapid activation of these factors that are essential for the melanization response to proceed, which could explain why single cSP gene knockdowns failed to rescue cSPH cleavage during systemic infections [10]. To address this question, we chose to characterize the cleavage pattern of CLIPA8 *in vitro*. The cleavage of full-length CLIPA8 was enhanced *in vivo* with *SRPN2* kd [10], and it was observed that SRPN2 directly inhibits the protease activities of CLIPB4, B9 and B10 [35, 37, 42]. This renders these three proteases as potential candidates for CLIPA8 cleavage. To that purpose, we expressed as recombinant form two versions of full-length CLIPA8; a wildtype version containing two C-terminal tags, V5 and His (CLIPA8-V5-His) and a mutant version in which the predicted cleavage site IMLR (cleavage predicted to occur after the R residue [6]) was replaced with IEGR (CLIPA8$_{Xa}$-V5-His) to allow cleavage by commercial Factor Xa. Both versions were obtained with high purity (minimally 95%) at ~ 54 kDa, and reacted with antibodies against CLIPA8, V5 and His as expected (online suppl. Fig S3). The theoretical weight of recombinant CLIPA8 is ~40 kDa based on the constructed plasmid pOET3-CLIPA8-V5-His, suggesting that the observed size shift is likely caused by protein modifications in the eukaryotic cell expression system.

Zymogens proCLIPB4$_{Xa}$-His, proCLIPB9$_{Xa}$-His and proCLIPB10$_{Xa}$-His containing a C-terminal His were expressed and purified as previously described [35, 37, 41]. Factor Xa was used to activate these three zymogens, and cleaved products corresponding to active CLIPB4$_{Xa}$ (Fig. 4a), CLIPB9$_{Xa}$ (Fig. 4b) and CLIB10$_{Xa}$ (Fig. 4c) were detected by western blot analyses using anti-His antibody. *In vitro* assays revealed that CLIPA8-V5-His was efficiently cleaved by Factor Xa-activated CLIPB4$_{Xa}$ (Fig. 4a), CLIPB9$_{Xa}$ (Fig. 4b) and CLIB10$_{Xa}$ (Fig. 4c). Cleaved CLIPA8 was detected at the same size as that of cleaved CLIPA8$_{Xa}$, suggesting that CLIPB4, B9 and B10 likely cleave CLIPA8 after the R residue in IMLR. Minimal cleavage of CLIPA8 was observed when incubated alone with proCLIPB4$_{Xa}$-His (Fig. 4a) or proCLIPB10$_{Xa}$-His (Fig. 4c), suggesting these CLIPB zymogens might have been minimally activated during purification. Altogether, our results suggest that cSPs may exhibit redundancy with respect to the cleavage of cSPHs in the core module.

CLIPB4 and CLIPB17 are central players in the melanization response to Gram-negative and Gram-positive bacteria

Two models of melanization have been largely adopted in *An. gambiae* to assess the roles of candidate CLIPBs in this response: the melanization of *P. berghei* ookinetes in *CTL4* kd refractory mosquitoes, and melanotic tumor formation triggered spontaneously in *SRPN2* kd naïve mosquitoes. These two models identified roles for CLIPB4, CLIPB8, CLIPB9, CLIPB10, CLIPB14 and CLIPB17 in the melanization response [33, 35-37, 41]. However, the implication of these CLIPBs in melanization triggered by microbes have thus far not been addressed. This is especially important, given the more significant evolutionary pressure that is likely to be imposed by bacteria and fungi, on the mosquito immune system, especially in their larval habitats. In contrast, only a small percentage of mosquitoes in the field are infected with *Plasmodium* parasites and there is no evidence that mosquito immunity genes have been subject to selection by malaria parasites [49, 50]. To gauge the contribution of the candidate CLIPBs in bacterial melanization, we used the Melanization-associated Spot Assay (MelASA) which quantifies melanin in mosquito excreta collected on Whatman filter paper as an indirect measure of hemolymph PO activity [34]. Silencing CLIPB4 and CLIPB17 but not CLIPB8, CLIPB9, CLIPB10 or CLIPB14 significantly reduced the total spot area of melanin deposits at 12 h after mosquito injections with low (OD_{600}=0.8) or high (OD_{600}=3) doses of *E. coli* compared to ds*LacZ* controls (Fig. 5a). However, the knockdown of neither of these CLIPBs reduced the total melanin spot area after *S. aureus* infections (Fig. 5b). To determine whether the phenotype observed with *S. aureus* spans other Gram-positive bacteria, we challenged mosquitoes with *M. luteus*, a low-virulence Gram-positive bacteria widely used in insect immune challenges [25, 51-53] and that is known to be a potent trigger of mosquito melanization [52, 54]. Our results revealed that all tested CLIPBs, except CLIPB14, significantly contribute to the melanization response triggered by *M. luteus* (Fig. 5c). On the other hand, *SPCLIP1* silencing almost abolished melanin excreta in response to all bacterial infections (Fig. 5), further supporting the central, non-redundant role the core cSPH module plays in the mosquito melanization response.

CLIPB14 regulates mosquito tolerance but not resistance to bacterial infections

Clip domain serine protease cascades regulate several key insect immune responses, including melanization, coagulation and Toll-signaling pathway. Certain catalytic cSPs in these

cascades function at the crossroads of PPO and Toll pathway activation [1, 29, 32], and silencing key immune-related cSPs in *Drosophila* increased the fly susceptibility to microbial infections [1, 27, 55]. We therefore tested whether any of our candidate CLIPBs contribute to mosquito tolerance and/or resistance to systemic bacterial infections. Tolerance, an indicator of host fitness to infection, was measured by scoring the survival of *CLIPB4*, *CLIPB8*, *CLIPB9*, *CLIPB10*, *CLIPB14* and *CLIPB17* kd mosquitoes after intrathoracic injections with *S. aureus* or *E. coli*. *CTL4* [56, 57] and *Rel1* [58] kd mosquitoes were used as positive controls for *E. coli* and *S. aureus* infections, respectively. Only *CLIPB14* kd compromised mosquito survival to infections with *E. coli* (Fig. 6c) and *S. aureus* (Fig. 6d), whereas silencing the other CLIPBs showed no effect on mosquito tolerance (Fig. 6a-d). Of note, the compromised survival of *CLIPB14* kd mosquitoes was only observed at low (OD_{600}=0.8) but not high (OD_{600}=2) infection doses. We utilized two different infection doses in these survival assays, since a previous study in *Drosophila* showed that the fly's survival to low and high doses of *S. aureus* infections relies on distinct immune responses [1]. Mosquito resistance, an indicator of immune-mediated microbial clearance, to *E. coli* and *S. aureus* systemic infections was measured by scoring the CFUs in whole mosquito homogenates prepared at 24 hrs post-bacterial intrathoracic injections. Interestingly, silencing neither of the CLIPBs influenced the ability of mosquitoes to clear either bacteria from the tissues (Fig. 6e-f). The same phenotype was also observed for *Rel1* kd, which is in line with our previous study [58], suggesting that Toll pathway might not be essential to *S. aureus* clearance at that time point post-infection.

Discussion

In this study, we provide novel insight into the hierarchical organization of the serine protease network that regulates mosquito melanization and the functional interactions between cSPs and cSPHs in this network. Our strategy capitalizes on characterizing the activation cleavage of cSPs *in vivo* as readouts to build hierarchy, as we have done with cSPHs [10]. However, we were only able to observe a cleavage profile for CLIPB10. The depletion of CLIPB8 from the hemolymph in response to infection suggests that it could be a node in the network on which several proteases converge leading to complete activation. This complete activation was not associated, however, with the detection of a cleaved product in the hemolymph, possibly because the active protein is either stably associated with microbial surfaces, since melanization is a highly

localized reaction, or that it is rapidly cleared from the hemolymph after inactivation by serpins. As for CLIPB4 and CLIPB9, we could not detect any activation profile (either cleavage or protein loss) in the hemolymph that could be used as a readout of protein activation. This suggests that, upon infection, only a small fraction of these proteins is activated and is either rapidly cleared by serpins and/or entrapped on microbial surfaces during melanin formation. This is in contrast to the cleaved products of most cSPHs which seem to be stable in the hemolymph and more easily detected [10, 11, 13], possibly because they lack enzymatic activity and hence clearance by serpins.

Epistasis analysis combined with western blotting revealed that CLIPB4 and CLIPB17 act upstream of CLIPB8, but they also control CLIPB10 cleavage independent of CLIPB8, indicating that downstream of CLIPB4 and CLIPB17, the cascade bifurcates into two branches; one converging on CLIPB8 and the other on CLIPB10. A bifurcation in the serine protease cascade regulating melanization has been well described in *M. sexta*, whereby downstream of the cSP HP21 two main branches emerge, one branch controls PAP3 activation while the second controls PAP1 in addition to Toll pathway activation [32]. The functional significance of the bifurcation downstream of CLIPB4/B17 is not clear yet, especially that CLIPB10 but not CLIPB8 has been shown to function as a PAP by directly activating PPO *in vitro* [37, 41]. It has been proposed that CLIPB8 functions upstream of CLIPB9, based on their non-redundant roles in *SRPN2* kd melanotic tumor formation and the ability of CLIPB9 to directly cleave PPO, acting as a PAP, but CLIPB8 cannot cleave CLIPB9 directly [41].

One of the intriguing observations that emerged from studying these protease cascades in *An. gambiae* is that none of the cSPs involved in melanization has been shown to individually control the activation cleavage of members of the core cSPH module in the hemolymph [10, 34]. Yet, insect cSPs, specifically PAPs, are known to cleave key cSPHs during the melanization response [38-40]. The fact that CLIPB4, CLIPB9, and CLIPB10 were able to efficiently cleave CLIPA8 *in vitro*, yet when silenced individually they previously failed to rescue the *in vivo* cleavage of CLIPA28, which is just downstream of CLIPA8 in the cSPH module [10], suggests that functional redundancy could mask certain interactions in the context of *in vivo* genetic studies. Based on our data we propose the following updated model of PPO activation in *An. gambiae* (Fig. 7). Upon infection, TEP1, the most upstream factor in the network [10, 12, 34], triggers the activation of the cSPH module through an unknown mechanism. A yet to be

identified ModSp, in turn, activates the cSP module, the most upstream member of which seems to be CLIPC9 as it controls the activation of CLIPB8 and CLIPB10 (this study), and most likely of CLIPB4 and CLIPB17, although this remains to be verified. Whether ModSp is activated by interacting with TEP1or another PRR remains to be elucidated. The hierarchy of CLIPCs with respect to CLIPBs in these cascades has been previously observed in several model insects (reviewed in [3, 4]). CLIPB4 seems to be a central player in the cSP module acting on multiple substrates, including CLIPA8 of the core cSPH module, CLIPB8 and PPO (this study and Zhang *et al*. this issue). Zhang *et al.* have recently shown that in addition to cleaving PPO, CLIPB4 also cleaves CLIPB8 *in vitro* [42], in agreement with our observations that *CLIPB4* kd rescues CLIPB8 depletion from the hemolymph in response to bacterial infections. We propose that bidirectional interactions between cSPs and cSPHs are essential for efficient PPO activation. Initially, systemic infection triggers low-level activation of cSPs, multiple members of which eventually cleave and activate members of the core cSPH module [SPCLIP1-CLIPA8-CLIPA28], as observed by CLIPA8 *in vitro* cleavage. Active cSPHs, in turn, induce signal amplification, possibly by serving as cofactors or adaptors that may facilitate cSP-cSP and cSP-PPO interactions in the protease cascade. The RNAi phenotypes of these core cSPHs characterized by complete abolishment of PO activity and melanin formation [10, 12, 13, 33, 34], support their central roles in the protease cascade. The role of cSPHs as cofactors for PPO activation is known in other model insects [38-40, 59], however, our work provides evidence, for the first time, that they also regulate cSP activation by showing that silencing any of the core cSPHs, SPCLIP1, CLIPA8 or CLIPA28, completely rescued CLIPB10 cleavage and CLIPB8 depletion from the hemolymph. The mechanism by which these cSPHs regulate cSP activation and the identity of their direct cSP targets awaits future studies.

The central, non-redundant role of cSPHs in melanization is also evident in the *SPCLIP1* kd phenotype in MelASA that almost completely abolished melanin formation in response to all bacterial challenges, whereas, the knockdown of candidate cSPs resulted in partial phenotypes. Among the cSPs, CLIPB4 and CLIPB17 seem to be central players as they significantly contribute to melanin formation in response to *E. coli* and *M. luteus* infections, however, the contributions of CLIPB8, B9, and B10 were only evident in the context of *M. luteus* infections. It seems that lyophilized suspensions of *M. luteus* triggered a more potent melanization response (as inferred from the total spot area in Fig. 5), allowing to better gauge the relative contributions

of cSPs. In support of this argument, the melanization response elicited against *M. luteus* in *Aedes aegypti* mosquitoes is stronger than that against *E. coli* [52, 60]. In our hands, *S. aureus* was not a good infection model for measuring the contributions of cSPs to melanization, possibly because this bacterium is rapidly and efficiently phagocytosed by hemocytes in mosquitoes [60, 61]. In contrast to their roles in melanization, none of the candidate CLIPBs was essential for bacterial clearance from the hemocoel. This was not surprising since the core cSPHs that play more central roles in melanization do not show significant contributions to bacterial clearance [10, 13], a process that is likely regulated by other effector responses including phagocytosis, antimicrobial peptides and those mediated by TEP1 and the CTL4-CTLMA2 C-type lectin complex [14, 43, 57, 61, 62]. On the other hand, CLIPB14 was the only candidate that was required for mosquito survival to low dose infections with *E. coli* and *S. aureus*, in agreement with its previously reported role [36]. This is an interesting phenotype, especially because CLIPB14 is not involved in melanization, suggesting that it could be part of the cascade that converges on the activation of the Toll pathway, which remains poorly characterized in mosquitoes. The recent publication of an antimicrobial activity assay to probe the Toll pathway may be used in the future to characterize the protease cascade that regulates Spaetzle cleavage and Toll pathway activation in *An. gambiae* [63].

In conclusion, our work has provided new insight into the structural organization and interaction of cSPs and cSPHs in the protease network that regulates mosquito melanization. The hierarchical structure we propose should guide future studies that employ targeted *in vitro* reconstitution assays and *in vivo* genetic studies to further refine the interactions in the network and unravel the logic behind its complex molecular organization.

Acknowledgement

We thank Kamal A. Shair Central Research Laboratory for providing free access to their equipment. K.M., X.Z., and B.M. would like to thank all members of the Michel laboratory for mosquito rearing and Dr. Michael Kanost (Kansas State University) for continued support and access to equipment for recombinant protein expression. We also thank Dr. Michael Povelones (University of Pennsylvania) for providing the CLIPC9 antibody.

Statement of Ethics

This study was carried according to the recommendations in the Guide for the Care and Use of Laboratory Animals of the National Institutes of Health (Bethesda, USA). Animal protocol was approved by the Institutional Animal Care and Use committee IACUC of the American University of Beirut (permit number 18-08-504). The IACUC functions in compliance with the Public Health Service Policy on the Humane Care and Use of Laboratory Animals (USA), and adopts the Guide for the Care and Use of Laboratory Animals of the National Institutes of Health.

Conflict of Interest Statement

The authors have no conflicts of interest to declare

Funding Sources

This work was supported by the National Institutes of Health, National Institute for Allergy and Infectious Disease, grant R01 AI140760 (to K.M. and M.A.O) and by the AUB Research Board award numbers 104107 and 104261 (to M.A.O.). The funding sources had no role in the preparation of data or the manuscript.

Author Contributions

Conceptualization and study design: Mike A. Osta and Kristin Michel. Experimental work: Sally A. Saab, Xiufeng Zhang, Bianca Morejon Viteri. Writing-original draft: Mike A. Osta, Sally A. Saab, and Xiufeng Zhang. Writing-review and editing: Mike A. Osta, Kristin Michel, Xiufeng Zhang and Bianca Morejon.

Data availability statement

All data generated or analyzed during this study are included in this article. Further inquiries can be directed to the corresponding author.

References

1. Dudzic JP, Hanson MA, Iatsenko I, Kondo S, Lemaitre B. More Than Black or White: Melanization and Toll Share Regulatory Serine Proteases in Drosophila. Cell Rep. 2019;27(4):1050-61 e3.

2. Veillard F, Troxler L, Reichhart JM. Drosophila melanogaster clip-domain serine proteases: Structure, function and regulation. Biochimie. 2016;122:255-69.
3. Kanost MR, Jiang H. Clip-domain serine proteases as immune factors in insect hemolymph. Curr Opin Insect Sci. 2015;11:47-55.
4. Nakhleh J, El Moussawi L, Osta MA. The melanization response in insect immunity. In: Ligoxygakis P, editor. Insect Immunity. Advances in Insect Physiology. 52: Elsevier; 2017. p. 2-20.
5. Povelones M, Osta MA, Christophides GK. The complement system of malaria vector mosquitoes. In: Raikhel AS, editor. Progress in Mosquito Research. Advances in Insect Phsyiology: Elsevier Ltd; 2016. p. 223-42.
6. Cao X, Gulati M, Jiang H. Serine protease-related proteins in the malaria mosquito, Anopheles gambiae. Insect Biochem Mol Biol. 2017;88:48-62.
7. Chen XG, Jiang X, Gu J, Xu M, Wu Y, Deng Y, et al. Genome sequence of the Asian Tiger mosquito, Aedes albopictus, reveals insights into its biology, genetics, and evolution. Proc Natl Acad Sci U S A. 2015;112(44):E5907-15.
8. Neafsey DE, Waterhouse RM, Abai MR, Aganezov SS, Alekseyev MA, Allen JE, et al. Mosquito genomics. Highly evolvable malaria vectors: the genomes of 16 Anopheles mosquitoes. Science. 2015;347(6217):1258522.
9. Waterhouse RM, Kriventseva EV, Meister S, Xi Z, Alvarez KS, Bartholomay LC, et al. Evolutionary dynamics of immune-related genes and pathways in disease-vector mosquitoes. Science. 2007;316(5832):1738-43.
10. El Moussawi L, Nakhleh J, Kamareddine L, Osta MA. The mosquito melanization response requires hierarchical activation of non-catalytic clip domain serine protease homologs. PLoS Pathog. 2019;15(11):e1008194.
11. Nakhleh J, Christophides GK, Osta MA. The serine protease homolog CLIPA14 modulates the intensity of the immune response in the mosquito Anopheles gambiae. J Biol Chem. 2017;292(44):18217-26.
12. Povelones M, Bhagavatula L, Yassine H, Tan LA, Upton LM, Osta MA, et al. The CLIP-Domain Serine Protease Homolog SPCLIP1 Regulates Complement Recruitment to Microbial Surfaces in the Malaria Mosquito Anopheles gambiae. PLoS Pathog. 2013;9(9):e1003623.
13. Schnitger AK, Kafatos FC, Osta MA. The Melanization Reaction Is not Required for Survival of *Anopheles gambiae* Mosquitoes after bacterial Infections. J Biol Chem. 2007;282(30):21884-8.
14. Yassine H, Kamareddine L, Chamat S, Christophides GK, Osta MA. A serine protease homolog negatively regulates TEP1 consumption in systemic infections of the malaria vector Anopheles gambiae. J Innate Immun. 2014;6(6):806-18.
15. Yassine H, Kamareddine L, Osta MA. The mosquito melanization response is implicated in defense against the entomopathogenic fungus Beauveria bassiana. PLoS Pathog. 2012;8(11):e1003029.
16. Simoes ML, Dong Y, Mlambo G, Dimopoulos G. C-type lectin 4 regulates broad-spectrum melanization-based refractoriness to malaria parasites. PLoS Biol. 2022;in press.
17. Simoes ML, Mlambo G, Tripathi A, Dong Y, Dimopoulos G. Immune Regulation of Plasmodium Is Anopheles Species Specific and Infection Intensity Dependent. MBio. 2017;8(5).

18. Ross J, Jiang H, Kanost MR, Wang Y. Serine proteases and their homologs in the Drosophila melanogaster genome: an initial analysis of sequence conservation and phylogenetic relationships. Gene. 2003;304:117-31.
19. Jin Q, Wang Y, Hartson SD, Jiang H. Cleavage activation and functional comparison of Manduca sexta serine protease homologs SPH1a, SPH1b, SPH4, and SPH101 in conjunction with SPH2. Insect Biochem Mol Biol. 2022;144:103762.
20. Kwon TH, Kim MS, Choi HW, Joo CH, Cho MY, Lee BL. A masquerade-like serine proteinase homologue is necessary for phenoloxidase activity in the coleopteran insect, *Holotrichia diomphalia* larvae. Eur J Biochem. 2000;267(20):6188-96.
21. Lee KY, Zhang R, Kim MS, Park JW, Park HY, Kawabata S, et al. A zymogen form of masquerade-like serine proteinase homologue is cleaved during pro-phenoloxidase activation by Ca2+ in coleopteran and *Tenebrio molitor* larvae. Eur J Biochem. 2002;269(17):4375-83.
22. Yu XQ, Jiang H, Wang Y, Kanost MR. Nonproteolytic serine proteinase homologs are involved in prophenoloxidase activation in the tobacco hornworm, Manduca sexta. Insect Biochem Mol Biol. 2003;33(2):197-208.
23. Buchon N, Poidevin M, Kwon HM, Guillou A, Sottas V, Lee BL, et al. A single modular serine protease integrates signals from pattern-recognition receptors upstream of the Drosophila Toll pathway. Proc Natl Acad Sci U S A. 2009;106(30):12442-7.
24. Jang IH, Chosa N, Kim SH, Nam HJ, Lemaitre B, Ochiai M, et al. A Spatzle-processing enzyme required for toll signaling activation in Drosophila innate immunity. Dev Cell. 2006;10(1):45-55.
25. Kambris Z, Brun S, Jang IH, Nam HJ, Romeo Y, Takahashi K, et al. Drosophila immunity: a large-scale in vivo RNAi screen identifies five serine proteases required for Toll activation. Curr Biol. 2006;16(8):808-13.
26. El Chamy L, Leclerc V, Caldelari I, Reichhart JM. Sensing of 'danger signals' and pathogen-associated molecular patterns defines binary signaling pathways 'upstream' of Toll. Nat Immunol. 2008;9(10):1165-70.
27. Issa N, Guillaumot N, Lauret E, Matt N, Schaeffer-Reiss C, Van Dorsselaer A, et al. The Circulating Protease Persephone Is an Immune Sensor for Microbial Proteolytic Activities Upstream of the Drosophila Toll Pathway. Mol Cell. 2018;69(4):539-50 e6.
28. Wang Y, Jiang H. Reconstitution of a branch of the Manduca sexta prophenoloxidase activation cascade in vitro: snake-like hemolymph proteinase 21 (HP21) cleaved by HP14 activates prophenoloxidase-activating proteinase-2 precursor. Insect Biochem Mol Biol. 2007;37(10):1015-25.
29. An C, Ishibashi J, Ragan EJ, Jiang H, Kanost MR. Functions of Manduca sexta hemolymph proteinases HP6 and HP8 in two innate immune pathways. J Biol Chem. 2009;284(29):19716-26.
30. An C, Jiang H, Kanost MR. Proteolytic activation and function of the cytokine Spatzle in the innate immune response of a lepidopteran insect, Manduca sexta. FEBS J. 2010;277(1):148-62.
31. Gorman MJ, Wang Y, Jiang H, Kanost MR. Manduca sexta hemolymph proteinase 21 activates prophenoloxidase-activating proteinase 3 in an insect innate immune response proteinase cascade. J Biol Chem. 2007;282(16):11742-9.
32. Wang Y, Yang F, Cao X, Zou Z, Lu Z, Kanost MR, et al. Hemolymph protease-5 links the melanization and Toll immune pathways in the tobacco hornworm, Manduca sexta. Proc Natl Acad Sci U S A. 2020;117(38):23581-7.

33. Volz J, Muller HM, Zdanowicz A, Kafatos FC, Osta MA. A genetic module regulates the melanization response of *Anopheles* to *Plasmodium*. Cell Microbiol. 2006;8(9):1392-405.
34. Sousa GL, Bishnoi R, Baxter RHG, Povelones M. The CLIP-domain serine protease CLIPC9 regulates melanization downstream of SPCLIP1, CLIPA8, and CLIPA28 in the malaria vector Anopheles gambiae. PLoS Pathog. 2020;16(10):e1008985.
35. An C, Budd A, Kanost MR, Michel K. Characterization of a regulatory unit that controls melanization and affects longevity of mosquitoes. Cell Mol Life Sci. 2011;68(11):1929-39.
36. Volz J, Osta MA, Kafatos FC, Muller HM. The Roles of Two Clip Domain Serine Proteases in Innate Immune Responses of the Malaria Vector *Anopheles gambiae*. J Biol Chem. 2005;280(48):40161-8.
37. Zhang X, Li M, El Moussawi L, Saab S, Zhang S, Osta MA, et al. CLIPB10 is a Terminal Protease in the Regulatory Network That Controls Melanization in the African Malaria Mosquito Anopheles gambiae. Front Cell Infect Microbiol. 2021;10:585986.
38. Wang Y, Jiang H. A positive feedback mechanism in the Manduca sexta prophenoloxidase activation system. Insect Biochem Mol Biol. 2008;38(8):763-9.
39. Wang Y, Lu Z, Jiang H. Manduca sexta proprophenoloxidase activating proteinase-3 (PAP3) stimulates melanization by activating proPAP3, proSPHs, and proPOs. Insect Biochem Mol Biol. 2014;50:82-91.
40. Kim MS, Baek MJ, Lee MH, Park JW, Lee SY, Soderhall K, et al. A new easter-type serine protease cleaves a masquerade-like protein during prophenoloxidase activation in *Holotrichia diomphalia* larvae. J Biol Chem. 2002;277(42):39999-40004.
41. Zhang X, An C, Sprigg K, Michel K. CLIPB8 is part of the prophenoloxidase activation system in Anopheles gambiae mosquitoes. Insect Biochem Mol Biol. 2016;71:106-15.
42. Zhang X, Zhang S, Kuang J, Sellens KA, Morejon B, Saab SA, et al. CLIPB4 is a central node in the protease network that regulates humoral immunity in Anopheles gambiae mosquitoes. bioRxiv. 2023:2023.07.07.545904.
43. Blandin S, Moita LF, Kocher T, Wilm M, Kafatos FC, Levashina EA. Reverse genetics in the mosquito *Anopheles gambiae*: targeted disruption of the Defensin gene. EMBO Rep. 2002;3(9):852-6.
44. Labrousse A, Chauvet S, Couillault C, Kurz CL, Ewbank JJ. Caenorhabditis elegans is a model host for Salmonella typhimurium. Curr Biol. 2000;10(23):1543-5.
45. Kamareddine L, Fan Y, Osta MA, Keyhani NO. Expression of trypsin modulating oostatic factor (TMOF) in an entomopathogenic fungus increases its virulence towards Anopheles gambiae and reduces fecundity in the target mosquito. Parasit Vectors. 2013;6:22.
46. Michel K, Budd A, Pinto S, Gibson TJ, Kafatos FC. *Anopheles gambiae* SRPN2 facilitates midgut invasion by the malaria parasite *Plasmodium berghei*. EMBO Rep. 2005;6(9):891-7.
47. Mendes AM, Schlegelmilch T, Cohuet A, Awono-Ambene P, De Iorio M, Fontenille D, et al. Conserved mosquito/parasite interactions affect development of *Plasmodium falciparum* in Africa. PLoS Pathog. 2008;4(5):e1000069.
48. Kan H, Kim CH, Kwon HM, Park JW, Roh KB, Lee H, et al. Molecular control of phenoloxidase-induced melanin synthesis in an insect. J Biol Chem. 2008;283(37):25316-23.
49. Crawford JE, Bischoff E, Garnier T, Gneme A, Eiglmeier K, Holm I, et al. Evidence for population-specific positive selection on immune genes of Anopheles gambiae. G3 (Bethesda). 2012;2(12):1505-19.

50. Rottschaefer SM, Riehle MM, Coulibaly B, Sacko M, Niare O, Morlais I, et al. Exceptional diversity, maintenance of polymorphism, and recent directional selection on the APL1 malaria resistance genes of Anopheles gambiae. PLoS Biol. 2011;9(3):e1000600.
51. Fuse N, Okamori C, Okaji R, Tang C, Hirai K, Kurata S. Transcriptome features of innate immune memory in Drosophila. PLoS Genet. 2022;18(10):e1010005.
52. Hillyer JF, Schmidt SL, Christensen BM. Rapid phagocytosis and melanization of bacteria and *Plasmodium* sporozoites by hemocytes of the mosquito *Aedes aegypti*. J Parasitol. 2003;89(1):62-9.
53. Kajla MK, Andreeva O, Gilbreath TM, 3rd, Paskewitz SM. Characterization of expression, activity and role in antibacterial immunity of Anopheles gambiae lysozyme c-1. Comp Biochem Physiol B Biochem Mol Biol. 2010;155(2):201-9.
54. Hillyer JF, Schmidt SL, Christensen BM. Hemocyte-mediated phagocytosis and melanization in the mosquito *Armigeres subalbatus* following immune challenge by bacteria. Cell Tissue Res. 2003;313(1):117-27.
55. Ligoxygakis P, Pelte N, Hoffmann JA, Reichhart JM. Activation of *Drosophila* Toll during fungal infection by a blood serine protease. Science. 2002;297(5578):114-6.
56. Dekmak AS, Yang X, Zu Dohna H, Buchon N, Osta MA. The Route of Infection Influences the Contribution of Key Immunity Genes to Antibacterial Defense in Anopheles gambiae. J Innate Immun. 2020:1-20.
57. Schnitger AK, Yassine H, Kafatos FC, Osta MA. Two C-type lectins cooperate to defend *Anopheles gambiae* against Gram-negative bacteria. J Biol Chem. 2009;284(26):17616-24.
58. Zakhia R, Osta MA. CLIPA7 Exhibits Pleiotropic Roles in the Anopheles gambiae Immune Response. J Innate Immun. 2022:1-16.
59. Ji Y, Lu T, Zou Z, Wang Y. Aedes aegypti CLIPB9 activates prophenoloxidase-3 in the presence of CLIPA14 after fungal infection. Front Immunol. 2022;13:927322.
60. Hillyer JF, Schmidt SL, Christensen BM. The antibacterial innate immune response by the mosquito *Aedes aegypti* is mediated by hemocytes and independent of Gram type and pathogenicity. Microbes Infect. 2004;6(5):448-59.
61. Moita LF, Wang-Sattler R, Michel K, Zimmermann T, Blandin S, Levashina EA, et al. *In vivo* identification of novel regulators and conserved pathways of phagocytosis in *A. gambiae*. Immunity. 2005;23(1):65-73.
62. Levashina EA, Moita LF, Blandin S, Vriend G, Lagueux M, Kafatos FC. Conserved role of a complement-like protein in phagocytosis revealed by dsRNA knockout in cultured cells of the mosquito, *Anopheles gambiae*. Cell. 2001;104(5):709-18.
63. Morejon B, Michel K. A zone-of-inhibition assay to screen for humoral antimicrobial activity in mosquito hemolymph. Front Cell Infect Microbiol. 2023;13:891577.

Figure legends

Fig. 1. CLIPB8 and CLIPB10 hemolymph proteins respond to microbial infection. CLIPB8 is consumed in the hemolymph in response to (**a**) *B. bassiana* and (**b**) *S. aureus*, but not (**c**) *E. coli* infection. CLIPB10 is cleaved at 24 hours after (**e**) *S. aureus* but not (**d**) *B. bassiana* nor (**f**) *E. coli* infections. Western blots of hemolymph extracts obtained at the indicated time points from (**a,d**) *B. bassiana* (2000 spores/mosquito), (**b,e**) *S. aureus* and (**c,f**) *E. coli* injected mosquitoes and probed with αCLIPB8. Western blots were probed with (**a-c**) αCLIPB8 and (**d-f**) αCLIPB10**,** respectively. All hemolymph samples were extracted from 40 mosquitoes, quantified using Bradford protein quantification assay, and equal amounts of protein were loaded into each well. Membranes were reprobed with αAPOII (without stripping) to control for loading. The figures shown are representative of 3 independent biological experiments. *C*, control naïve mosquitoes.

Fig. 2. CLIPB4 and CLIPB17 act upstream of CLIPB8 and CLIPB10 in the serine protease cascade regulating melanization. Western blots showing (**a**) CLIPB8 protein levels and (**b**) CLIPB10 cleavage profile in the hemolymph of mosquitoes treated with the indicated gene-specific double-stranded (ds) RNA at 10 and 24 hrs after *S. aureus* infection, respectively. Two representative trials are shown per experiment. All hemolymph samples were extracted from 40 mosquitoes, quantified using Bradford protein quantification assay, and equal protein amounts were loaded into each well. Membranes were reprobed with αAPOII (without stripping) as loading control. **c** Schematic diagram showing the hierarchical organization of SPCLIP1 with respect to the catalytic CLIPBs in the melanization response to systemic bacterial infections. CLIPB4 and CLIPB17 are shown in a rectangular box because their respective hierarchies have not been determined. Dashed lines indicate that the enzymatic steps are not yet fully characterized.

Fig. 3. TEP1 and the core cSPH module control the activation of CLIPB8 and CLIPB10. Western blots showing (**a**) CLIPB10 cleavage profile and (**b**) CLIPB8 protein levels in the hemolymph of mosquitoes treated with the indicated gene-specific double-stranded (ds) RNAs at 10 and 24 hrs after *S. aureus* infection, respectively. In (**a**), low (left) and extended (right) exposures of the same membrane are shown in order to reveal the CLIPB10-C band that is often

very weak. All hemolymph samples were extracted from 40 mosquitoes, quantified using Bradford protein quantification assay, and equal protein amounts were loaded into each well. Membranes were reprobed with αAPOII (without stripping) as loading control. The figures shown are representative of 3 independent biological experiments. **c** Schematic diagram showing the hierarchical organization of TEP1, the core cSPH module and the catalytic CLIPBs and CLIPC9 in the melanization response to systemic bacterial infections. Dashed lines indicate that the enzymatic steps are not yet fully characterized.

Fig. 4. Recombinant proCLIPA8 is cleaved by B4, B9 and B10 *in vitro*. Recombinant proCLIPA8-V5-His is cleaved by (**a**) Factor Xa-activated $B4_{Xa}$-His, (**b**) $B9_{Xa}$-His, and (**c**) $B10_{Xa}$-His at the predicted site, examined by Western blot analyses using anti-His and anti-V5 antibodies. Zymogens of CLIPB members were activated by Factor Xa, and incubated with wild-type proCLIPA8 for (**a**,**b**) 1 hour at RT or (**c**) 30 min on ice. The activation of corresponding CLIPB members by Factor Xa was included for each Western blot analysis. A positive control was included with Factor Xa-cleavage of $proCLIPA8_{Xa}$ for 2 hours at RT. Both anti-His and anti-V5 antibodies detected the cleaved fragment of wild-type proCLIPA8 at a similar size as that of Factor Xa-cleaved $proCLIPA8_{Xa}$. Solid and hollow arrows indicate the full-length and activated forms of CLIPB members, respectively; for $CLIPA8_{Xa}$, solid and hollow stars indicate the full-length and cleaved forms, respectively.

Fig. 5. CLIPB4 and CLIPB17 are central players in the melanization response to bacterial infections. MelASA assay conducted on the indicated mosquito genotypes at 12 hrs post (**a**) *E. coli*, (**b**) *S. aureus* and 18 hrs post (**c**) *M. luteus* infections. The amount of melanin deposits present in infected mosquito excreta was measured from Whatman papers placed at the bottom of the paper cups housing 35 (for *E. coli* and *S. aureus*) or 50 (for *M. luteus*) mosquitoes per sample. Statistical analysis was done using unpaired t-tests to compare two treatment groups, and One-Way ANOVA with Dunnett's post-test to compare multiple treatment groups. Means are shown in red lines. Data shown are from at least 6 independent trials. *, $P<0.05$; ***, $P<0.001$; ****, $P<0.0001$.

Fig. 6. CLIPB14 is required for mosquito tolerance but not resistance to bacterial infections. **a**-**b** Survival analysis of the indicated mosquito genotypes challenged with (**a** and **c**) *E. coli*, and (**b**

and **d**) *S. aureus*. A representative experiment of at least three independent trials is shown. The Kaplan-Meier survival test was used to calculate the percent survival. Statistical significance of the observed differences was calculated using the Log-rank test. *, $P<0.05$; **, $P<0.01$; ***, $P<0.001$; ****, $P<0.0001$. **e**-**f** Bacterial proliferation assays conducted on the indicated mosquito genotypes injected with (**e**) *E. coli* (OD_{600}=0.8) and (**f**) *S. aureus* (OD_{600}=0.8). Batches of 8 whole mosquitoes each were homogenized in LB medium at 24 hours post-infection and colony forming units (CFUs) were scored on LB plates supplemented with the appropriate antibiotic. Each point on the scatter plot represents the mean CFU per mosquito per batch. Statistical analysis was performed using Kruskal-Wallis test followed by Dunn's multiple comparisons test, with *P*-values less than 0.05 considered significant. Means are in red. *P*-values are shown only for samples that significantly differ from the control (ds*LacZ*). Data presented are from 4 independent experiments.

Fig. 7. Schematic drawing of the protease network regulating mosquito melanization. The scheme indicates the current knowledge of hierarchy in the cSP and cSPH modules constituting the network. Dashed lines indicate hierarchy inferred from genetic studies *in vivo* (i.e. hemolymph) described in this study (red) or previous work (black; [10, 12, 34, 41]). Solid lines indicate direct cleavage events inferred from *in vitro* assays described in this study (red), previous work (black; [35, 37]) or the companion paper of Zhang *et al*. in this issue (blue; [42]). Dashed, blue line represents the presumably promiscuous cleavage of members of the cSPH modules by several cSPs. The module serine protease (ModSp) that acts upstream of cSPs is shown in grey as its identity is still unknown in *An. gambiae*. Dashed lines indicate that the enzymatic steps are not yet fully characterized.

Figure 1

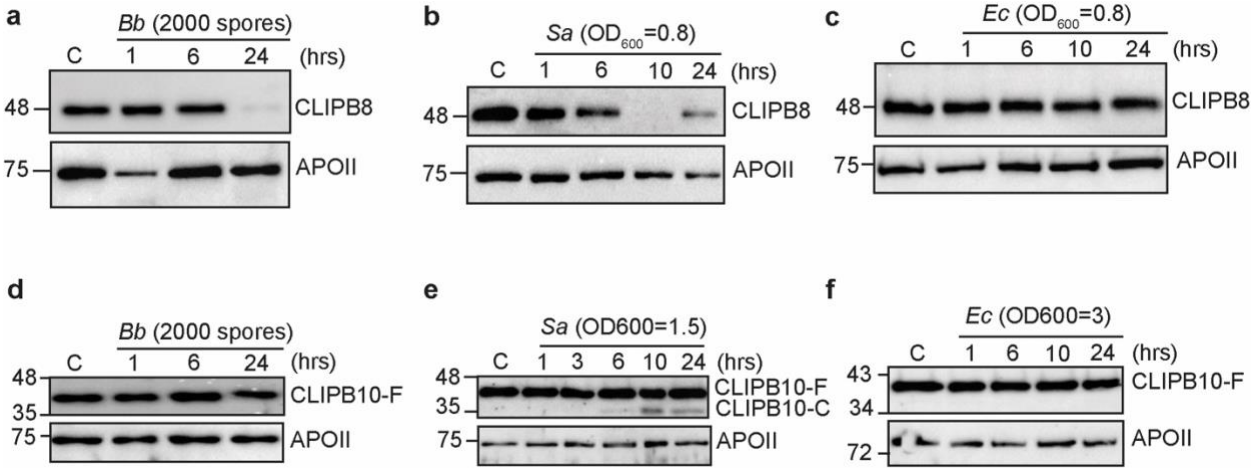
a
Bb (2000 spores)
C 1 6 24 (hrs)
48
CLIPB8
75
APOII
b
Sa (OD600=0.8)
C 1 6 10 24 (hrs)
48
CLIPB8
75
APOII
c
Ec (OD600=0.8)
C 1 6 10 24 (hrs)
48
CLIPB8
75
APOII
d
Bb (2000 spores)
C 1 6 24 (hrs)
48
35
CLIPB10-F
75
APOII
e
Sa (OD600=1.5)
C 1 3 6 10 24 (hrs)
48
35
CLIPB10-F
CLIPB10-C
75
APOII
f
Ec (OD600=3)
C 1 6 10 24 (hrs)
43
34
CLIPB10-F
72
APOII

Figure 2

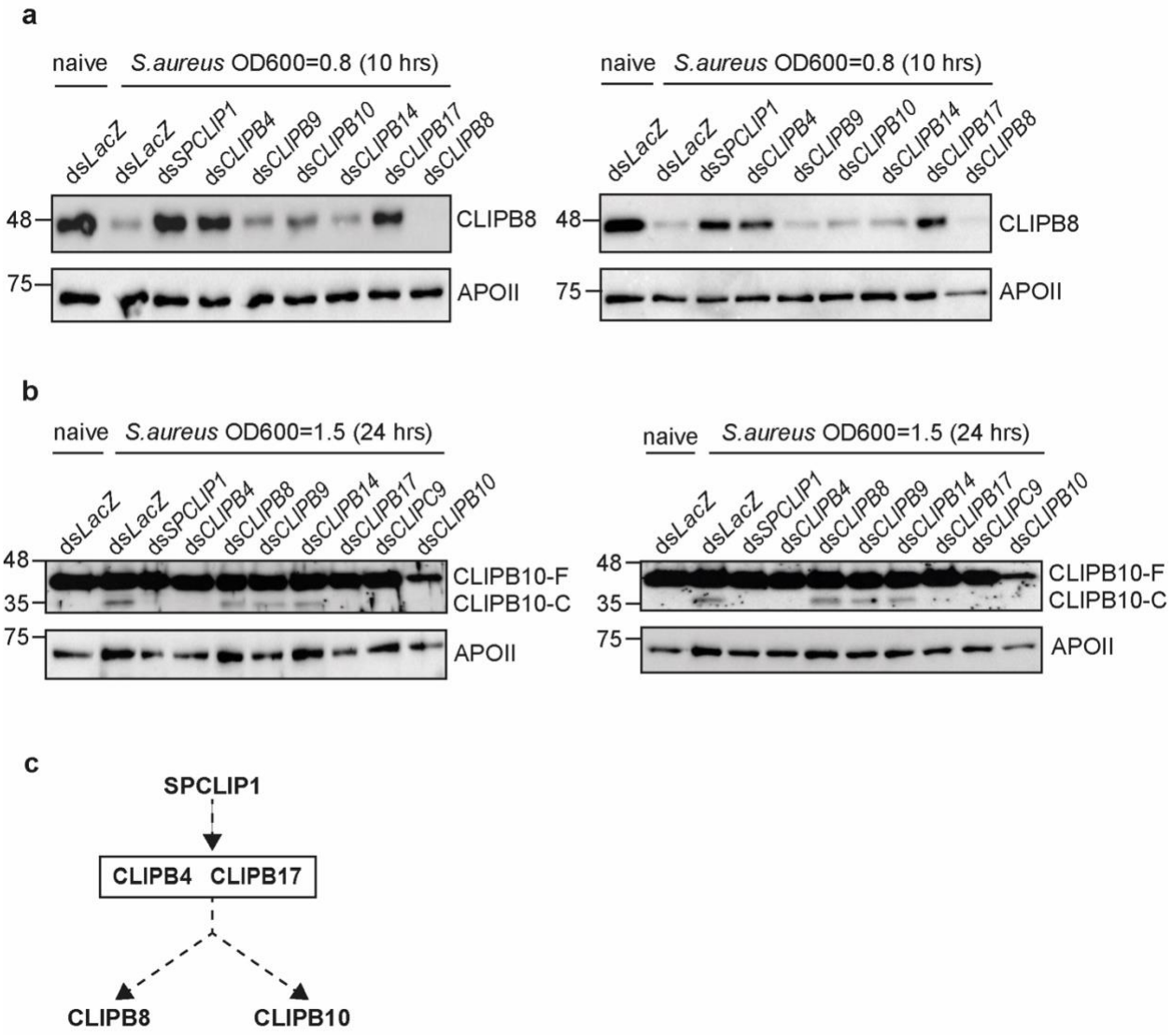
a
naive
S.aureus OD600=0.8 (10 hrs)
dsLacZ
dsLacZ
dsSPCLIP1
dsCLIPB4
dsCLIPB9
dsCLIPB10
dsCLIPB14
dsCLIPB17
dsCLIPB8
48
75
CLIPB8
APOII
naive
S.aureus OD600=0.8 (10 hrs)
dsLacZ
dsLacZ
dsSPCLIP1
dsCLIPB4
dsCLIPB9
dsCLIPB10
dsCLIPB14
dsCLIPB17
dsCLIPB8
48
75
CLIPB8
APOII
b
naive
S.aureus OD600=1.5 (24 hrs)
dsLacZ
dsLacZ
dsSPCLIP1
dsCLIPB4
dsCLIPB8
dsCLIPB9
dsCLIPB14
dsCLIPB17
dsCLIPC9
dsCLIPB10
48
35
75
CLIPB10-F
CLIPB10-C
APOII
naive
S.aureus OD600=1.5 (24 hrs)
dsLacZ
dsLacZ
dsSPCLIP1
dsCLIPB4
dsCLIPB8
dsCLIPB9
dsCLIPB14
dsCLIPB17
dsCLIPC9
dsCLIPB10
48
35
75
CLIPB10-F
CLIPB10-C
APOII
c
SPCLIP1
CLIPB4 CLIPB17
CLIPB8
CLIPB10

Figure 3

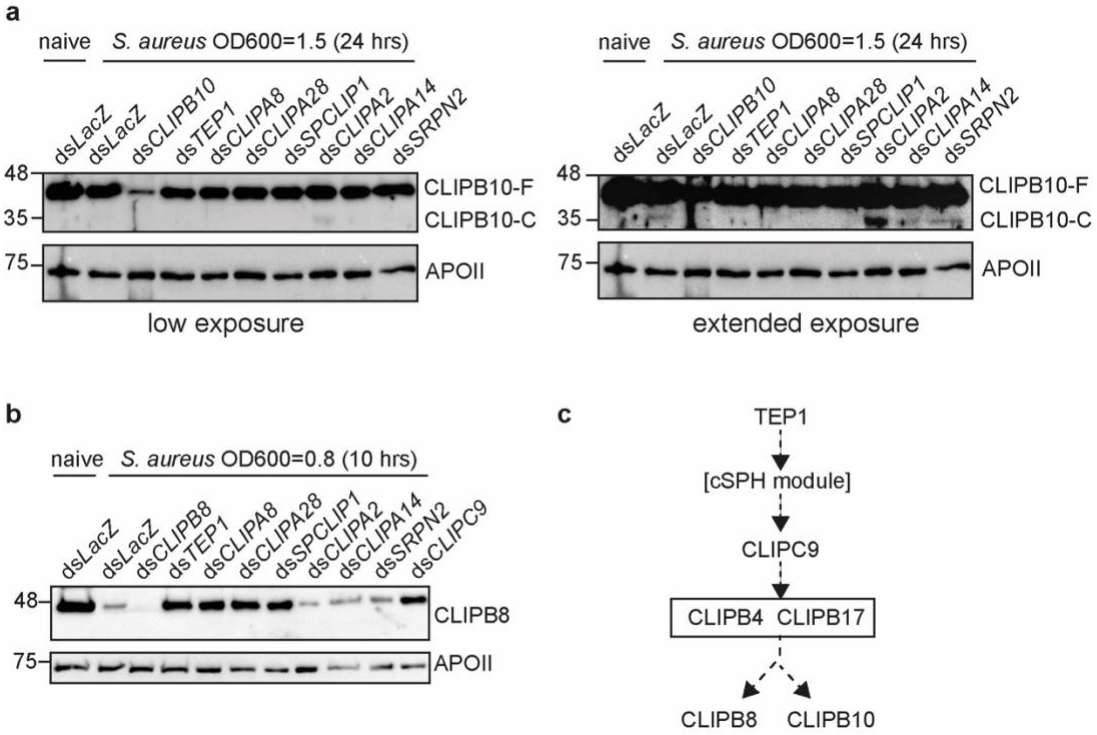
a
naive
S. aureus OD600=1.5 (24 hrs)
dsLacZ
dsLacZ
dsCLIPB10
dsTEP1
dsCLIPA8
dsCLIPA28
dsSPCLIP1
dsCLIPA2
dsCLIPA14
dsSRPN2
48
35
75
CLIPB10-F
CLIPB10-C
APOII
low exposure
extended exposure
b
naive
S. aureus OD600=0.8 (10 hrs)
dsLacZ
dsLacZ
dsCLIPB8
dsTEP1
dsCLIPA8
dsCLIPA28
dsSPCLIP1
dsCLIPA2
dsCLIPA14
dsSRPN2
dsCLIPC9
48
75
CLIPB8
APOII
c
TEP1
[cSPH module]
CLIPC9
CLIPB4 CLIPB17
CLIPB8
CLIPB10

Figure 4

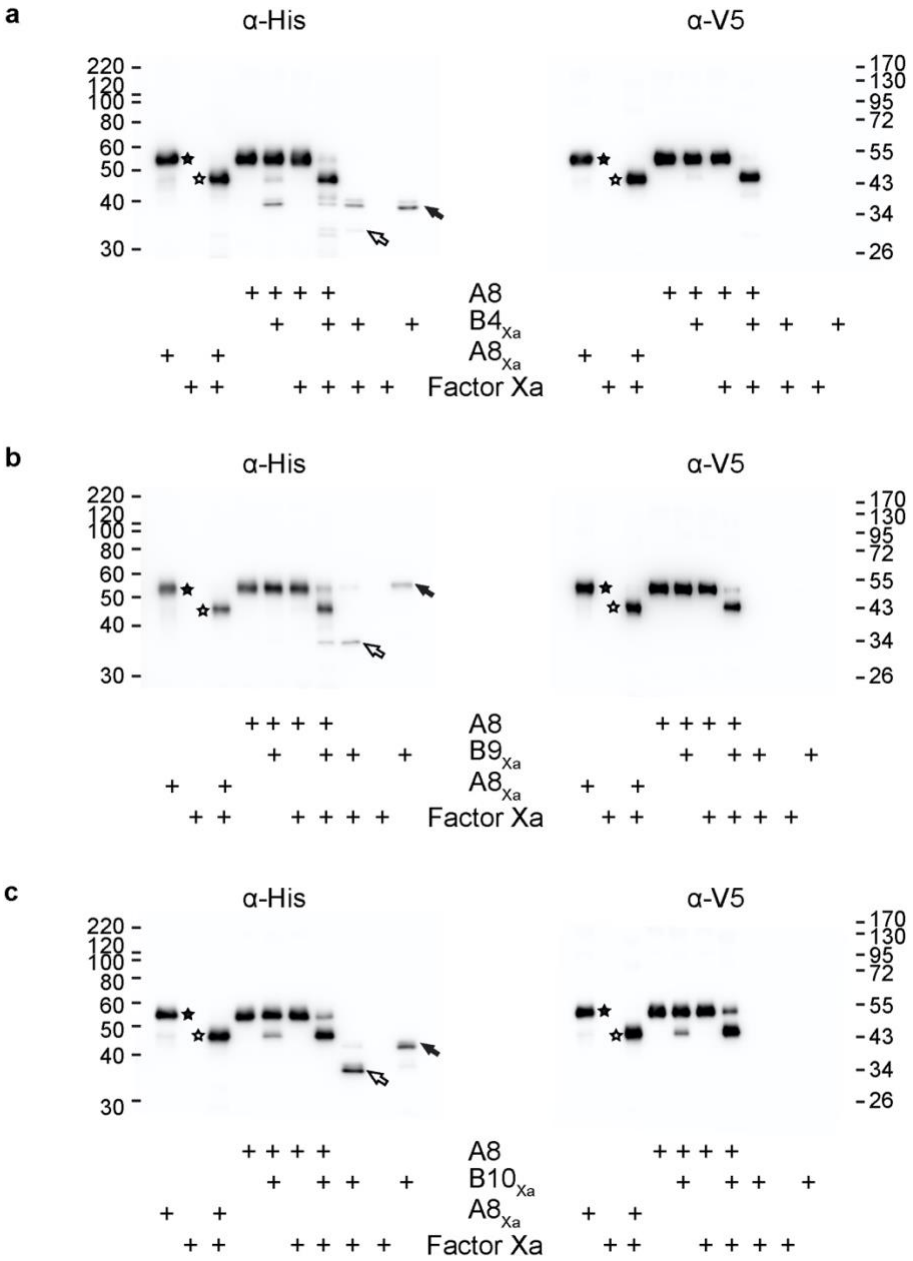
a
α-His
α-V5
220
120
100
80
60
50
40
30
170
130
95
72
55
43
34
26
A8
B4Xa
A8Xa
Factor Xa
b
α-His
α-V5
A8
B9Xa
A8Xa
Factor Xa
c
α-His
α-V5
A8
B10Xa
A8Xa
Factor Xa

Figure 5

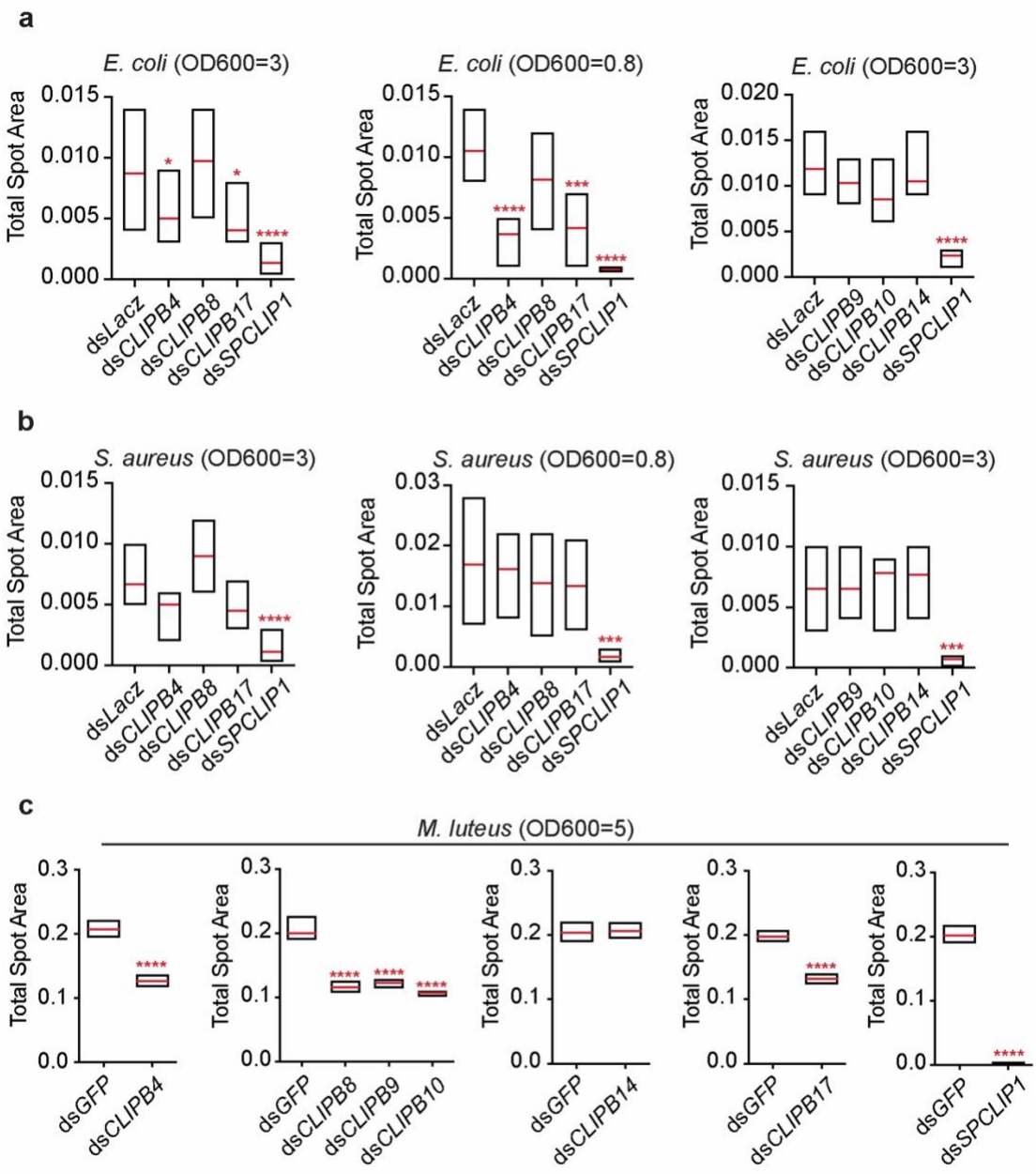
a
E. coli (OD600=3)
E. coli (OD600=0.8)
E. coli (OD600=3)
Total Spot Area
dsLacz
dsCLIPB4
dsCLIPB8
dsCLIPB17
dsSPCLIP1
dsCLIPB9
dsCLIPB10
dsCLIPB14
b
S. aureus (OD600=3)
S. aureus (OD600=0.8)
S. aureus (OD600=3)
c
M. luteus (OD600=5)
dsGFP

Figure 6

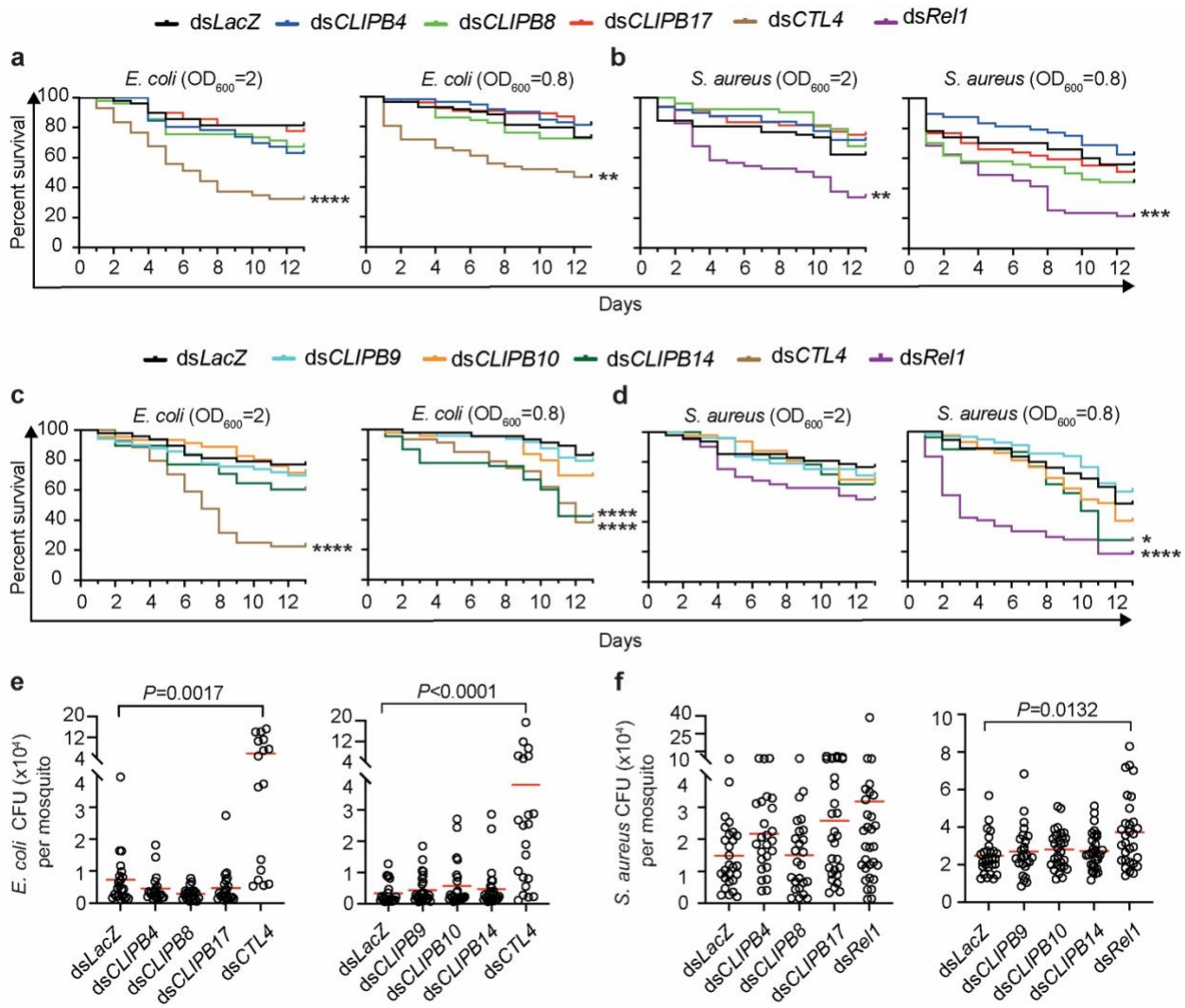
dsLacZ
dsCLIPB4
dsCLIPB8
dsCLIPB17
dsCTL4
dsRel1
a
b
E. coli (OD600=2)
E. coli (OD600=0.8)
S. aureus (OD600=2)
S. aureus (OD600=0.8)
Percent survival
Days
dsLacZ
dsCLIPB9
dsCLIPB10
dsCLIPB14
dsCTL4
dsRel1
c
d
E. coli (OD600=2)
E. coli (OD600=0.8)
S. aureus (OD600=2)
S. aureus (OD600=0.8)
Percent survival
Days
e
f
P=0.0017
P<0.0001
P=0.0132
E. coli CFU (x10⁴) per mosquito
S. aureus CFU (x10⁴) per mosquito
dsLacZ
dsCLIPB4
dsCLIPB8
dsCLIPB17
dsCTL4
dsCLIPB9
dsCLIPB10
dsCLIPB14
dsRel1

Figure 7

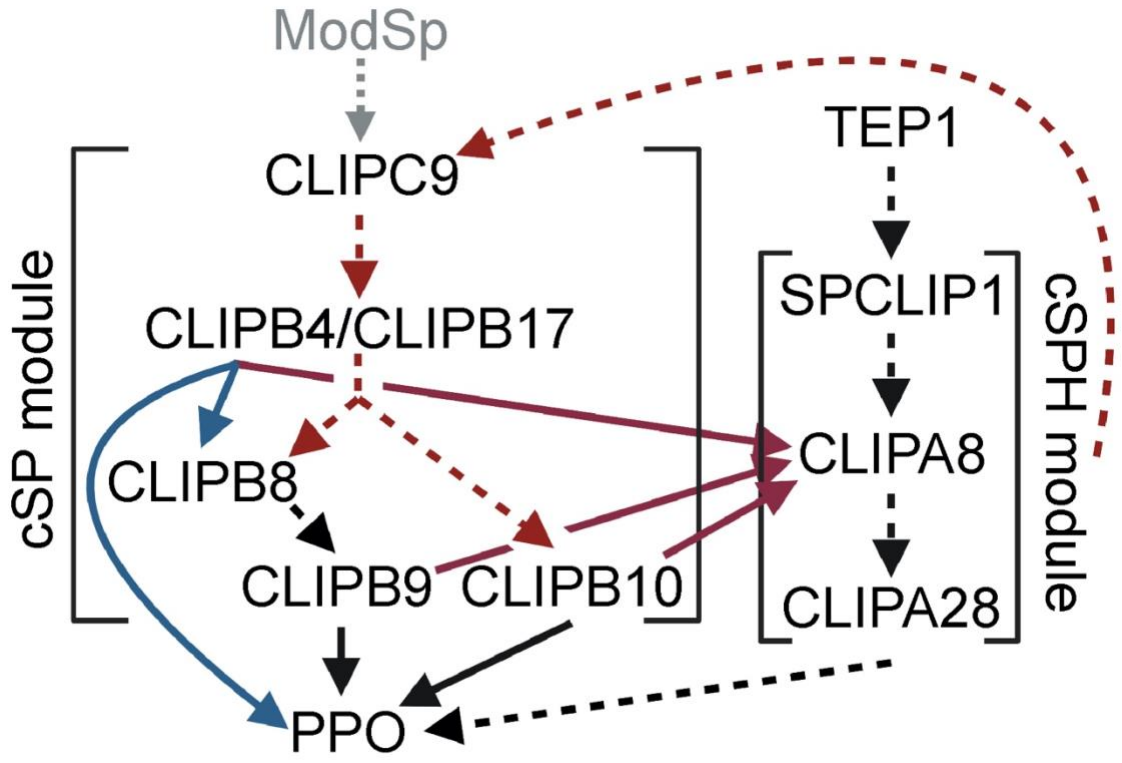
ModSp
CLIPC9
TEP1
cSP module
CLIPB4/CLIPB17
SPCLIP1
cSPH module
CLIPB8
CLIPA8
CLIPB9
CLIPB10
CLIPA28
PPO